Electronic Supplementary Material (ESI) for Nanoscale.

Supplementary Information

Super Hydrophilic $LaCoO_3$/g-C_3N_4 Nanocomposite Coated Beauty Sponge for Solar-driven Seawater Desalination with Simultaneous Volatile Organic Compound Removal

Lokesh Kumar Rathore,[a] *Parul Garg,*[a] *Piyush Kumar,*[b] *Ashok Bera**[a]

[a]Department of Physics, Indian Institute of Technology Jammu, J&K 181221, India

[b]Department of Chemistry, Indian Institute of Technology Jammu, J&K 181221, India

Corresponding author:

Dr. Ashok Bera*

Email: ashok.bera@iitjammu.ac.in

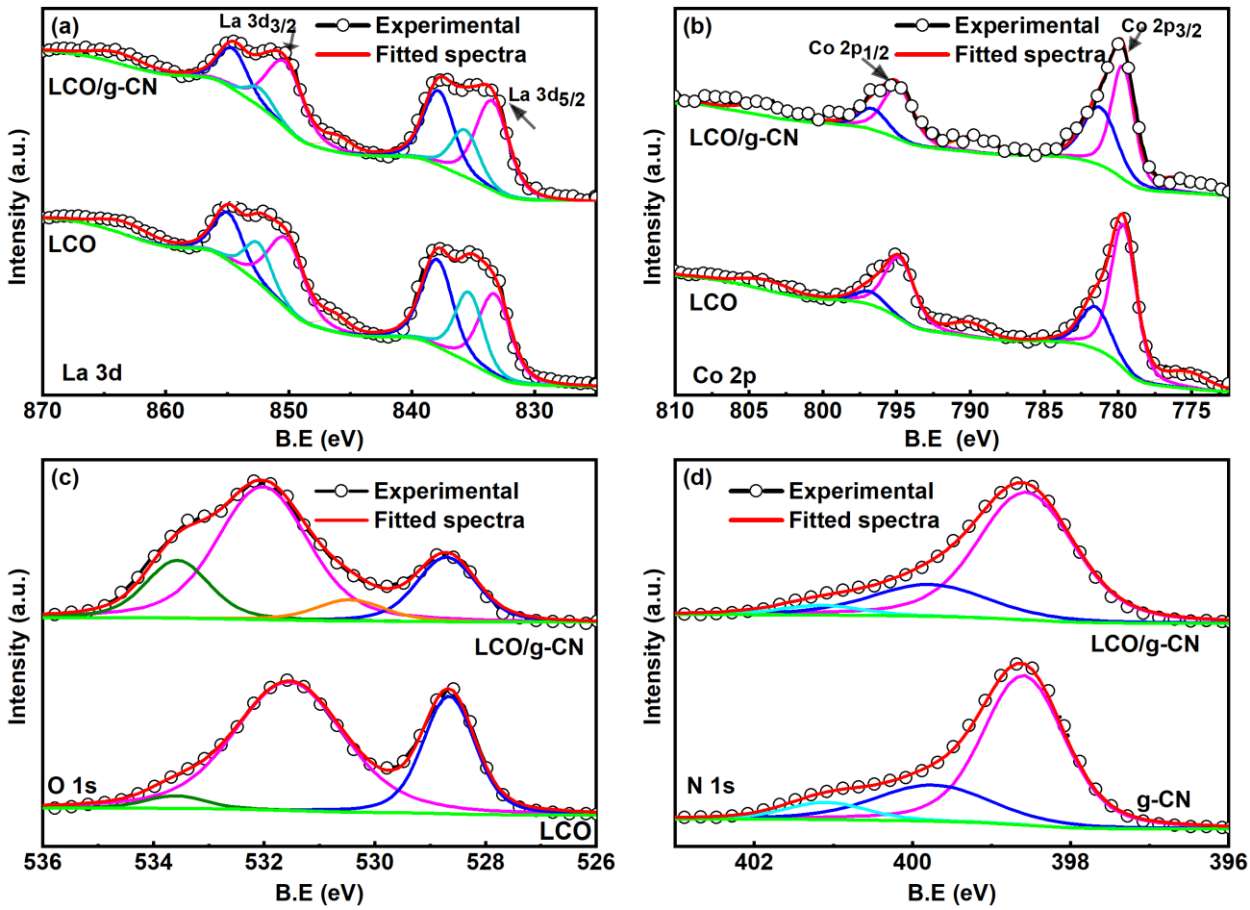

Fig. S1 High-resolution XPS spectra of (a) La 3d, (b) Co 2p, (c) O 1s, (d) N 1s for corresponding samples

Note S1: As shown in Figure S2a, the high-resolution La 3d XPS spectra of the LCO and LCO/g-CN samples exhibit two distinct shoulder peaks with shake-up features positioned within the 830−840 eV and 850−857 eV ranges. These can be deconvoluted into two prominent shoulder peaks at 833.61, and 837.6 eV and corresponding shakeup peaks at 850.08, and 854.8 eV, respectively, which were assigned to the orbitals of La $3d_{5/2}$ and La $3d_{3/2}$, respectively, confirming the occurrence of La^{3+} in the prepared samples.[1] For the high-resolution Co 2p spectra (Figure S2b), the peaks at about 780 and 795.18 eV can be assigned to Co $2p_{3/2}$ and Co $2p_{1/2}$ orbitals, while the broad low intense peaks centered at about 790 and 804.38 eV were the

satellite peaks of Co 2p. The Co $2p_{3/2}$ peak and Co $2p_{5/2}$ peak can be deconvoluted to two peaks at 779.28, 781.3 eV and 794.78 eV, and 796.58 eV for both samples, indicating the presence of Co^{2+} and Co^{3+} cations in LCO and LCO/g-CN, respectively.[2] Additional understanding of the interaction between LCO and g-CN is garnered from the O 1s core level spectrum. Figure S1c shows three distinct O 1s features: 528.68 eV indicates the oxygen on the surface of the materials (lattice oxygen), 531.5 eV represents the hydroxyl oxygen, and 533.6 eV corresponds to the surface adsorbed oxygen. In the LCO/g-CN nanocomposite, the surface oxygen content decreases, and the hydroxyl band position undergoes a 0.5 eV shift, indicating a change in its chemical atmosphere upon its interaction with LCO.[3] The high-resolution N 1s spectrum of the two samples shown in Figure S1d has been deconvoluted to three prominent peaks at 398.5 eV, 399.7 eV, and 401.3 eV corresponding to the sp^2 hybridized N in C═N─C bond, the one at 399.7 eV to the N atoms surrounded by three carbon atoms in g-CN and the weak peak at 401.3 eV indicated graphitic nitrogen.[4] Based on our XPS results, it is evident that a substantial number of C-N bonds exist between the N and C atoms in the prepared LCO/g-CN powder samples, facilitating the formation of the desired composite.

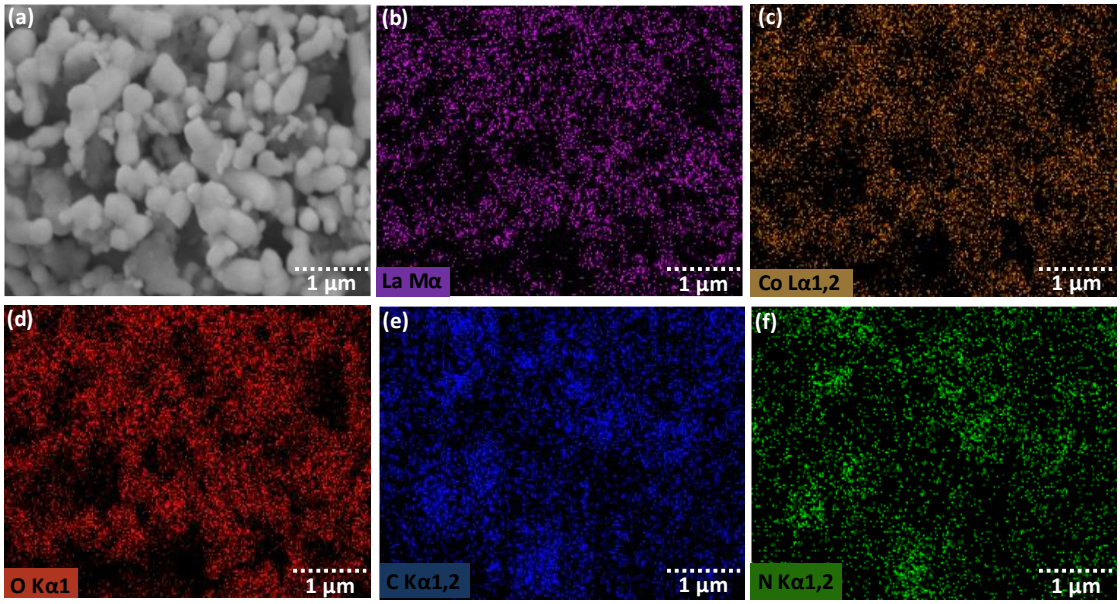

Fig. S2 (a) FESEM image of LCO/g-CN nanocomposite; corresponding EDS elemental graphs for (b) La (c) Co (d) O (d) C and (e) N.

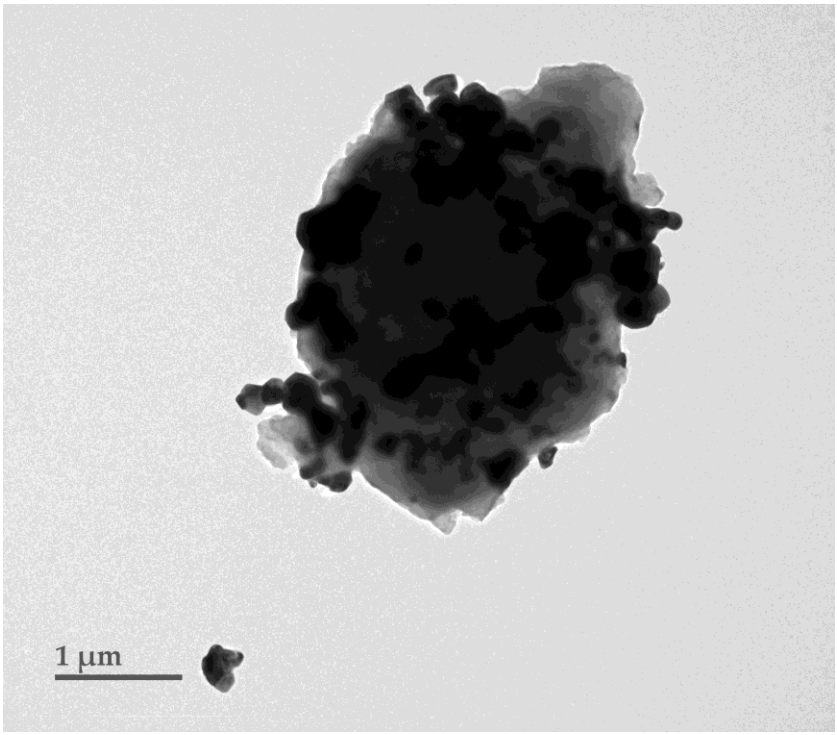

Fig. S3 TEM image of LCO/g-CN nanocomposite. It can be seen clearly in that the LCO nanoparticles are well attached to g-CN layered structure.

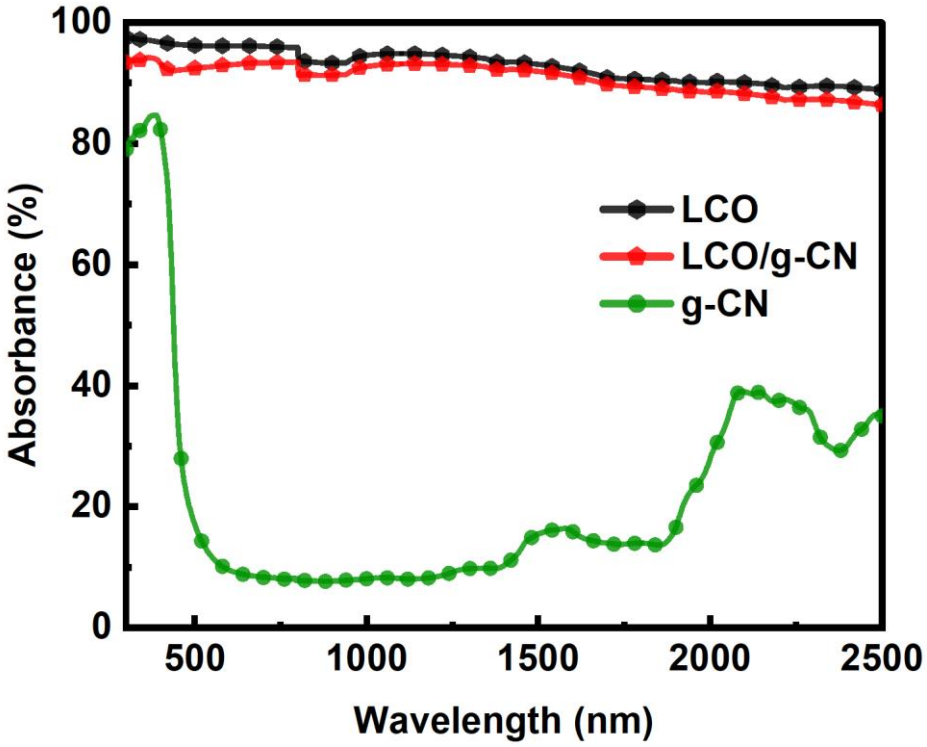

Fig. S4 UV-Vis-NIR absorption spectra of LCO, g-CN, and LCO/g-CN nanocomposite powders.

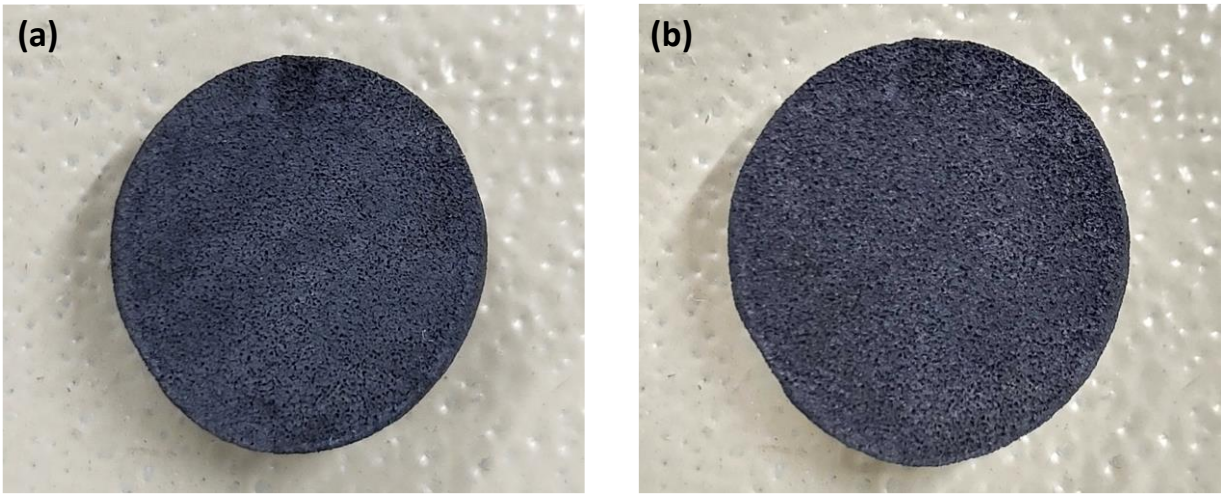

Fig. S5 Digital photographs of LCO/g-CN@BS in (a) the dry state and (b) the wet state

Table S1 Comparison of the evaporation rates with other recently reported evaporators

S. N.	Photothermal material	Solar intensity ($kW\ m^{-2}$)	Evaporation rate ($kg\ m^{-2}\ h^{-1}$)	Reference
1	Cu_3BiS_3@V_2C/BF	1.0	1.68	5
2	G@ZIF films	1.0	1.78	6
3	Cotton-CNT	1.0	1.59	7
4	MXene@rGO membrane	1.0	1.33	8
5	Biomass-based device	1.0	1.41	9
6	hierarchically structured hydrogel evaporators	1.0	1.77	10
7	Wood-Inspired Aerogel	1.0	1.54	11
8	graphene-supported MIL-125	1.0	1.26	12
9	sawdust-based composite	1.0	1.4	13
10	Ferric tannate hydrogel	1.0	1.53	14
11	Plasmonic nanoparticle-embedded poly(p-phenylene benzobisoxazole)	1.0	1.42	15
12	Polydopamine-filled bacterial nanocellulose	1.0	1.13	16
13	MoS2-coated wood	1.0	1.46	17
14	Chitosan aerogel-carbon nanotubes	1.0	1.55	18
15	Surface modified sponge	1.0	1.12	19
16	Bifunctional graphene aerogel	1.0	1.80	20
17	Acrylic paint	1.0	1.4	21
18	LCO/g-CN@BS	1.0	1.94	**This work**

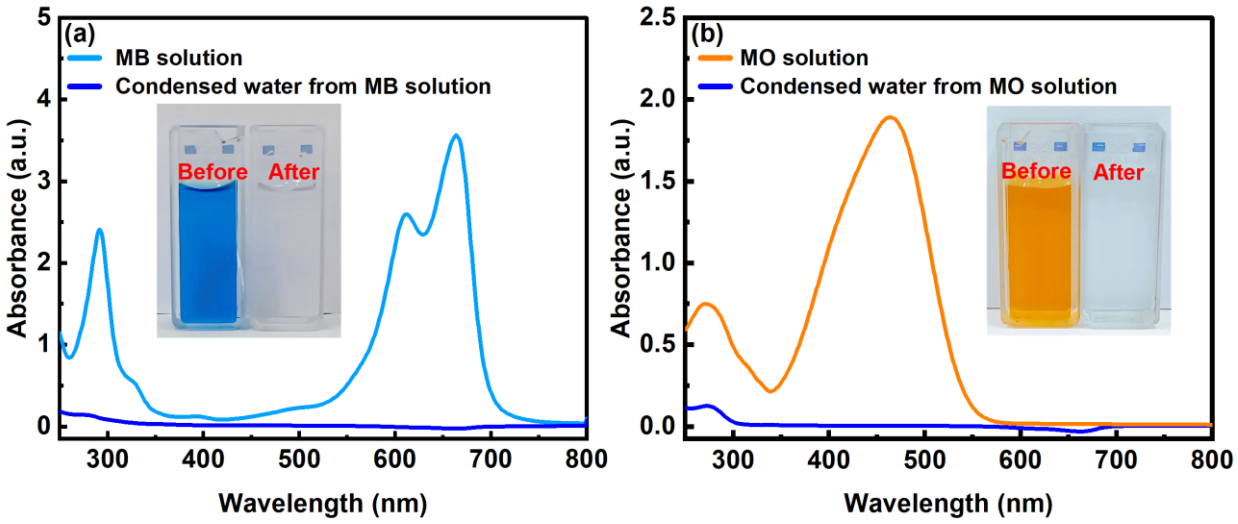

Fig. S6 UV-Vis absorption spectra before and after purification for (a) methylene blue (MB) solution and (b) methyl orange (MO) solution.

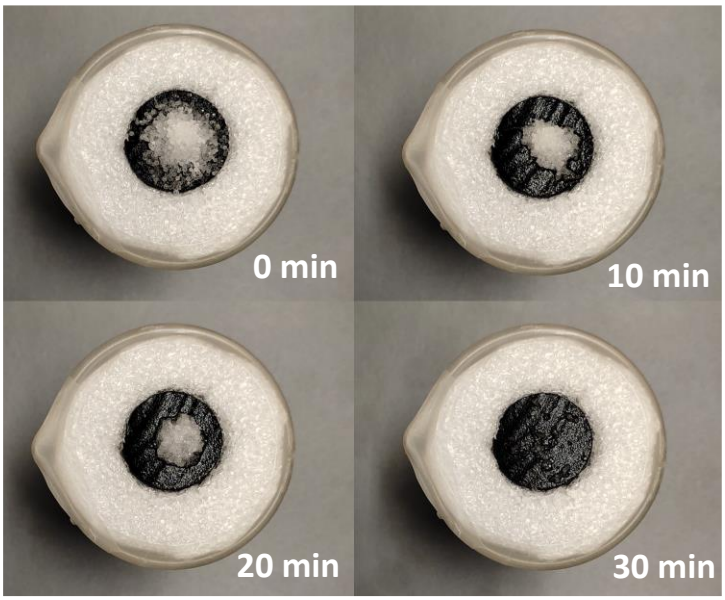

Fig. S7 Digital photographs of the self-cleaning ability experiment of LCO/g-CN@BS for salt. Typically,1 g of salt was placed on the top surface of LCO/g-CN@BS which was self-dissolved within 30 minutes.

Table S2 Comparison of the current work with other state-of-the-art evaporators.

S. N.	Photothermal material	Evaporation rate ($kg\ m^{-2}\ h^{-1}$)	VOC removal efficiency	Reference
1	BiOBrI decorated sponge	1.67	99% (5 mg/L)	22
2	CuFeMnO4/ceramic plate	1.45	98.2% (20 mg/L)	23
3	PPy membrane	1.12	90% (5 mg/L)	24
4	Alginate/carbon black SWEG	1.4	99% (100 ppm)	25
5	rGO-SA-TiO2	1.63	96% (2 mg/L)	26
6	m-TiO_{2-x}-NFM	1.71	95.5% (10 mg/L)	27
7	Nanofiber-constructed aerogel	1.88	95% (5 mg/L)	28
8	CTAB/carbon black	1.30	53.95% (10 mg/L)	29
9	TiO2-CuO-Cu foam	1.28	80% (25 mg/L)	30
10	LCO/g-CN@BS	1.94	92% (10 mg/L)	**This work**

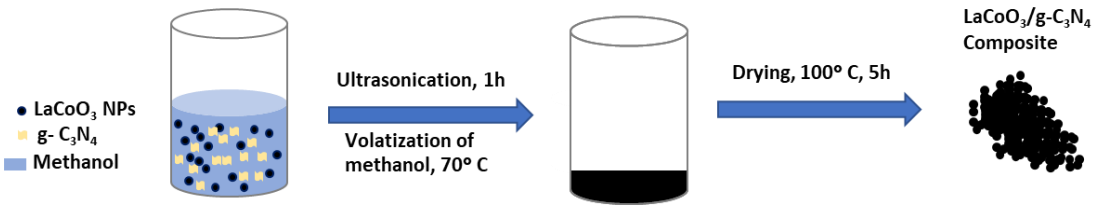

Fig. S8 Schematic illustration of the preparation of LCO/g-CN nanocomposite.

References

1 T. Ahmad Wani, P. Garg, S. Bera, S. Bhattacharya, S. Dutta, H. Kumar and A. Bera, *J. Colloid Interface Sci.*, 2022, **612**, 203–212.

2 C. Wang, L. Zeng, W. Guo, C. Gong and J. Yang, *RSC Adv.*, 2019, **9**, 35646–35654.

3 R. Wang, C. Ye, H. Wang and F. Jiang, *ACS Omega*, 2020, **5**, 30373–30382.

4 B. Ren, T. Wang, G. Qu, F. Deng, D. Liang, W. Yang and M. Liu, *Environ. Sci. Pollut. Res.*, 2018, **25**, 19122–19133.

5 R. Xu, H. Cui, N. Wei, J. Zhao, X. Song, Y. Han, J. Yang, A. Wang and M. Zhao, *Desalination*, 2024, **570**, 117094.

6 X. Han, L. V. Besteiro, C. S. L. Koh, H. K. Lee, I. Y. Phang, G. C. Phan-Quang, J. Y. Ng, H. Y. F. Sim, C. L. Lay, A. Govorov and X. Y. Ling, *Adv. Funct. Mater.*, 2021, **31**, 2008904.

7 H. Kou, Z. Liu, B. Zhu, D. K. Macharia, S. Ahmed, B. Wu, M. Zhu, X. Liu and Z. Chen, *Desalination*, 2019, **462**, 29–38.

8 P. Ying, B. Ai, W. Hu, Y. Geng, L. Li, K. Sun, S. C. Tan, W. Zhang and M. Li, *Nano Energy*, 2021, **89**, 106443.

9 Z. Xu, Y. Yang, W. Yao, C. Ye, H. Qiao, J. Shen and M. Ye, *ACS Appl. Mater. Interfaces*, 2023, **15**, 48336–48345.

10 W. Lei, S. Khan, L. Chen, N. Suzuki, C. Terashima, K. Liu, A. Fujishima and M. Liu, *Nano Res.*, 2021, **14**, 1135–1140.

11 Q. Zhang, Y. Chen, Y. Wang, J. He, P. Yang, Y. Wang and S. Tang, *ACS Appl. Mater. Interfaces*, 2023, **15**, 50522–50531.

12 O. R. Hayes, A. A. Ibrahim, M. S. Adly, S. E. Samra, A. M. A. Ouf, S. A. El-Hakam and A. I. Ahmed, *RSC Adv.*, 2023, **13**, 18525–18537.

13 M. Rengasamy and K. Rajaram, *RSC Adv.*, 2023, **13**, 5173–5184.

14 C. Zhang, Y. Jiang, X. Zou, L. Xing, W. Liu, Z. Huang, Y. Feng and J. Wang, *ACS Appl. Polym. Mater.*, 2023, **5**, 9574-9584.

15 M. Chen, Y. Wu, W. Song, Y. Mo, X. Lin, Q. He and B. Guo, *Nanoscale*, 2018, **10**, 6186–6193.

16 Q. Jiang, H. Gholami Derami, D. Ghim, S. Cao, Y. S. Jun and S. Singamaneni, *J. Mater. Chem. A*, 2017, **5**, 18397–18402.

17 X. He, L. Zhang, X. Hu and Q. Zhou, *Environ. Sci. Nano*, 2021, **8**, 2069–2080.

18 Q. Liu, W. Xiao, B. Liao, K. Yan and J. Zhang, *Chem. Eng. J. Adv.*, 2022, **10**, 100260.

19 Z. Zhang, P. Mu, J. He, Z. Zhu, H. Sun, H. Wei, W. Liang and A. Li, *ChemSusChem*,

2019, **12**, 426–433.

20 F. Wu, D. Liu, G. Li, L. Li, L. Yan, G. Hong and X. Zhang, *Nanoscale*, 2021, **13**, 5419–5428.

21 T. A. Wani, V. Gupta, P. Garg and A. Bera, *ACS Sustain. Chem. Eng.*, 2023, **11**, 9595–9600.

22 J. Ma, L. An, D. Liu, J. Yao, D. Qi, H. Xu, C. Song, F. Cui, X. Chen, J. Ma and W. Wang, *Environ. Sci. Technol.*, 2022, **56**, 9797–9805.

23 L. Shi, Y. Shi, S. Zhuo, C. Zhang, Y. Aldrees, S. Aleid and P. Wang, *Nano Energy*, 2019, **60**, 222–230.

24 D. Qi, Y. Liu, Y. Liu, Z. Liu, Y. Luo, H. Xu, X. Zhou, J. Zhang, H. Yang, W. Wang and X. Chen, *Adv. Mater.*, 2020, **32**, 1–9.

25 P. Zhang, F. Zhao, W. Shi, H. Lu, X. Zhou, Y. Guo and G. Yu, *Adv. Mater.*, 2022, **34**, 1–8.

26 W. Dong, Y. Wang, Y. Zhang, X. Song, H. Peng and H. Jiang, *Chem. - A Eur. J.*, 2021, **27**, 17428–17436.

27 C. Song, D. Qi, Y. Han, Y. Xu, H. Xu, S. You, W. Wang, C. Wang, Y. Wei and J. Ma, *Environ. Sci. Technol.*, 2020, **54**, 9025–9033.

28 M. Li, Z. Zhu, L. Ni, L. Qi, Y. Yang, Y. Zhou, J. Qi and J. Li, *ACS EST Engg.*, 2023, **3**, 2027-2037.

29 C. Li, X. Zhou, Y. Xiao, T. Zhang, M. *Sci. Total Environ.*, 2022, **815**, 152694.

30 Y. Tian, H. Yang, S. Wu, B. Gong, C. Xu, J. Yan, K. Cen, Z. Bo and K. Ostrikov, *Int. J. Energy Res.*, 2022, **46**, 1313–1326.